Nonlinear features and complexity patterns of vegetation dynamics in the transition zone of North China

Zhiqiang Zhao [a,b], Jianguo Liu [b], Jian Peng [a], Shuangcheng Li [a], Yanglin Wang [a,*]

[a] Laboratory for Earth Surface Processes Ministry of Education, College of Urban and Environmental Sciences, Peking University, Beijing 100871, China
[b] Center for Systems Integration and Sustainability, Department of Fisheries and Wildlife, MI State University, East Lansing, MI 48823, USA

ABSTRACT

Normalized Difference Vegetation Index (NDVI) has been commonly used to estimate terrestrial vegetation distribution and productivity. In this study, we adopted recurrence quantification analysis (RQA) to investigate the spatial patterns of determinism of the vegetation dynamics ecological-geographical transition zones in North China, especially the differences between transition zone and the surrounding areas. The results indicated that there were obvious regional variances in spatial patterns of RQA indices—determinism, laminarity, entropy, and averaged diagonal line length. Remarkable differences of the determinism of NDVI time series also existed between transition zones and the surrounding areas. Moreover, the correlation analysis between the RQA indices and climatic factors suggested that the determinism of the NDVI time series was nonlinearly affected by hydrothermal conditions. Influenced by vegetation patterns, determinism reached the maximum when the annual precipitation is about 400 mm, which is the lower bound of cultivation and forest distribution, and along the 400 mm isohyet is the area where transition zones locate.

© 2014 Elsevier Ltd. All rights reserved.

1. Introduction

Normalized Difference Vegetation Index (NDVI) has been commonly used as an estimator of terrestrial vegetation distribution and productivity (Kerr and Ostrovsky, 2003; Xiao and Moody, 2004; Evans et al., 2006; Davies et al., 2007). Since global climate change became a major topic of study, vegetation dynamics and the relationships between NDVI and climatic factors have become hot spots in academic research (Xiao and Moody, 2004; Piao et al., 2006; Xu et al., 2007; Guo et al., 2008; Luo et al., 2009; Udelhoven et al., 2009; Li et al., 2011). Several global and regional studies have used NDVI dataset to investigate the vegetation spatial-temporal characteristics (Moody and Johnson, 2001; Piao et al., 2003; Wu et al., 2009; Zhang et al., 2009) and how they relate to climatic factors (Fang et al., 2001; Piao et al., 2006; Onema and Taigbenu, 2009).

According to the Köppen climate classification (Kottek et al., 2006; Peel et al., 2007), ecological–geographical transition zones generally have semi-arid climates and exhibit some features of transition in ecological characteristics. Transition zones, known as fragile areas and sensitive to climate change, are widely distributed

around the world. Located at the northern edge of the East Asian monsoon influences, transition zones of North China are one of the important areas of global change research. Many researchers focused on the change pattern, process, and landscape ecological significance, and concentrated on the relationships between NDVI and climatic factors in this area (Liu et al., 2000, 2010; Li et al., 2006a; Guo et al., 2007; Cui et al., 2009; Liu and Cui, 2009; Wang et al., 2009; Wu et al., 2009; Zhang et al., 2011; Sun and Guo, 2012).

One of the key aims of studying the temporal and spatial features of regional climate and vegetation was to estimate future performance of climate change and vegetation dynamics, because forecasting is the premise of plans and decision making. To infer the future state of climate change and vegetation dynamics we need to study the dynamic features of historical processes. However, scientists have generally recognized that the process of climate systems and ecosystems is complex and nonlinear (Turchin and Taylor, 1992; Pascual and Ellner, 2000; Green et al., 2005; Pickett et al., 2005; Li et al., 2006b, 2008b, 2011; Zhao et al., 2011). Meanwhile, many studies have discovered that NDVI–environment relationships have some complex features such as nonlinearity, scale-dependency, and non-stationarity, especially in highly heterogeneous areas (Foody, 2004; Osborne et al., 2007; Li et al., 2011; Gao et al., 2012; Zhao et al., 2014). Some measures of nonlinear dynamics have been developed to estimate the complexity of nonlinear dynamic systems, such as the correlation

dimension, Lyapunov exponents, Kolmogorov entropy, approximate entropy, sample entropy, and permutation entropy (Torres and Gamero, 2000; Li et al., 2006b). In 1987, the method of recurrence plots (RPs) was introduced as another approach to describe complex dynamics (Eckmann et al., 1987; Zbilut and Webber, 1992; Webber and Zbilut, 1994; Marwan et al., 2007, 2009). More recently, the quantitative measure for RPs, recurrence quantification analysis (RQA), was introduced to bivariate and multivariate analyses of complex systems and successfully applied in various fields, such as biology (Webber and Zbilut, 1994; Webber et al., 2011), economics (Fabretti and Ausloos, 2005), ecology (Proulx et al., 2008, 2009; Li et al., 2011), and earth science (Marwan et al., 2003; Li et al., 2008b; Zhao et al., 2011). This also provides us with a tool for identifying the nonlinear features of vegetation dynamics. However, few studies have focused on the nonlinear dynamics features of vegetation in these transition zones.

Transition zones are the regional boundaries where climatic conditions and vegetation distributions gradually shift from one distinctive type to another. Transition zones have a relatively high level of complexity in spatial patterns and greater species diversity. A number of theoretical and experimental studies have confirmed the stabilising effects of ecosystem biodiversity across different spatial scales (Proulx et al., 2010; Allan et al., 2011; De Mazancourt et al., 2013). Basing on the diversity–stability hypothesis,

increasing landscape diversity could enhance ecosystem stability and reduce the temporal complexity of vegetation dynamics. We evaluated the determinism and temporal complexity of NDVI time-series inside and outside bio-climatic transition zones of North China to see whether the determinism of NDVI time-series was higher in transition zones. Additionally, we analyzed the correlation between the RQA indices and climatic factors to explore potential reasons for the complexity patterns of NDVI.

2. Materials and methodology

2.1. Study area

Our study area (35°–48°N, 102°–126°E) is located in North China. Its elevation ranges from 0 to 5007 m, with higher topography in the northwest and lower in the southeast. The climatic conditions are mainly dominated by the Pacific summer monsoon from the southeast and the winter monsoon from continental Inner Asia. Therefore, annual precipitation (AP) in this region decreases from the southeast to the northwest and ranges between less than 100 mm west of Inner Mongolia Plateau to >800 mm at the southeast coastal zone. The annual mean temperature (AMT) ranges from −10 °C to 15 °C. The vegetation patterns are associated with climatic conditions, chief among them moisture conditions. With decreasing AP from southeast to
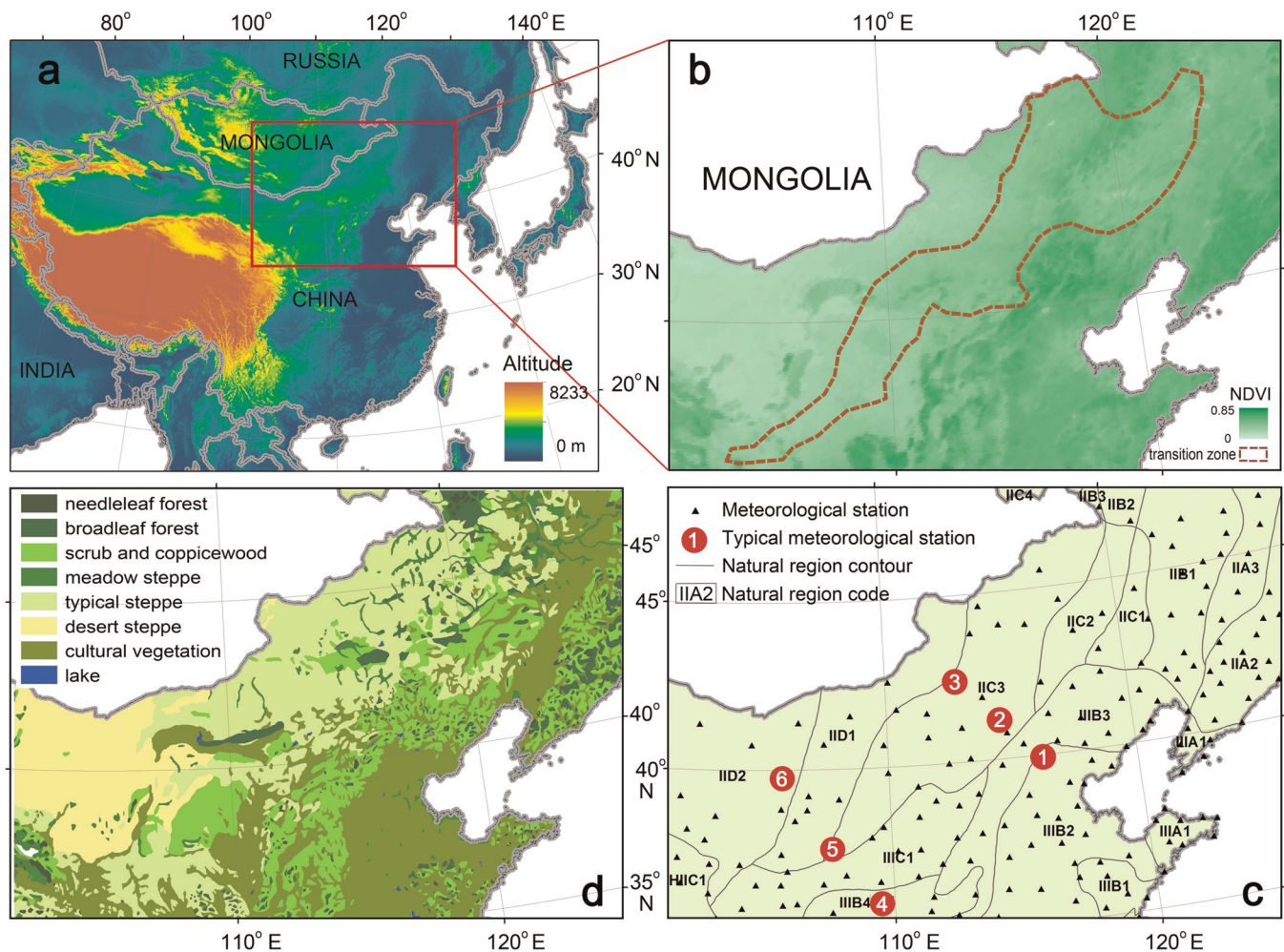

Fig. 1. Map of the study area. (a) Digital elevation map (DEM) of the study area (red rectangle) and surroundings; (b) NDVI map of the study area with the transition zone (red dashed line); (c) Meteorological stations and natural regions divisions of the study area; In nature region code, the Rome numbers represented division of temperature zone: II was sub temperate zone, III was Warm-temperate zone, and HII was Plateau temperate zone; the capital letter represented division of dry and wet areas: A was humid area, B was sub- humid area, C was sub-arid area, and D was arid area. (d) Study area showing vegetation patterns.

northwest, vegetation changes from agricultural land, forest, and shrubland (AP > ~400 mm), to meadow steppe (AP ~ 400–350 mm), to typical steppe (AP ~ 350–250 mm), and then to desert steppe (AP ~ 250–150 mm) (Fig. 1d).

With the vast size and diversity of climate and vegetation, this area can be divided into three temperature belts and sixteen natural regions (Fig. 1c) (Zheng, 2008). In this region, there is an important ecological–geographical transition zone where the semi-humid agriculture area and arid and semi-arid pasturing area meet. The transition zone is generally distributed along the 400 mm isohyet, a boundary between semi-humid monsoon climate and semi-arid continental climate. In the transition zone, the forest–steppe ecotone is distributed by islands of forest patches embedded on meadow steppe with AP ranging from 350 mm to 450 mm and is consistent with the mountain ranges. The forest patches are found only on shady, steep slopes (>20°) of hills or mountains (Liu et al., 2009, 2010). In this study, we defined the border of the ecological–geographical transition zone by using indexes including AP (~300–450 mm), rainfall variability (15% to ~~30%), and aridity index (1.0–2.0) (Fig. 1b), based on the combination of previous research (Wang et al., 1999; Zhao et al., 2002; Zheng, 2008).

2.2. Methods

Marwan et al. (2007) gave a detailed description of the principle and the algorithm of RPs and RQA. Hence, we give only a brief overview of RPs and RQA in this section. For more detailed descriptions, readers can refer to the article "Recurrence plots for the analysis of complex systems" (Marwan et al., 2007).

2.2.1. Recurrence plots and recurrence quantification analysis

RPs were first introduced to visualize recurrences of trajectories of dynamic systems in phase space (Eckmann et al., 1987). The RP was defined by

$$R_{i,j}(\varepsilon) = \Theta\left(\varepsilon - \parallel x_i - x_j \parallel\right) i, j = 1 \cdots N, \tag{1}$$

where N was the number of measured points x_i, ε was a small threshold distance, $\parallel \cdot \parallel$ was a norm, and $\Theta(\cdot)$ was the Heaviside function. By using Taken's time delay method $x_i = (u_i, u_{i+\tau}, \cdots, u_{i+(m-1)\tau})$ with embedding dimension m and delay time τ, the phase space vectors for one-dimensional observed time series u_i were generally reconstructed. The distance between two points, x_i and x_j, in the phase space trajectory is calculated to compare with a specified threshold ε. In a two-dimensional matrix, if $R_{i,j} \equiv 1$, the recurrence states at time i and time j could be marked by black points, and if $R_{i,j} \equiv 0$, it is marked by white points (Marwan and Kurths, 2005; Marwan et al., 2007; Li et al., 2008b).

Fig. 2 shows the RPs of three typical synthetic time series. Fig. 2a shows the homogeneous RPs' structure of stochastic series, characterized mainly by single points. Fig. 2b represents a sine function, i.e., a circle in phase space. Its RPs are then characterized by non-interrupted diagonal lines and indicate high DET (Von Bloh et al., 2005). Fig. 2c denotes the RPs of a sinusoidal sequence with white noise, and the patterns are between those shown in Figs. 2a and b.

To quantify the RPs, Zbilut and Webber developed RQA and defined indices, including the recurrence rate, determinism (DET), the averaged and maximal lengths of diagonal structures, and the Shannon entropy to measure the complexity based on the recurrence point density and diagonal line structures in the RPs (Zbilut and Webber, 1992; Webber and Zbilut, 1994). Subsequently, Marwan and Kurths (2002) extended the RQA by introducing two additional measures, laminarity and trapping time, which are based on the vertical structures in the RPs. The RQA method and these measures provide a powerful tool to analyze nonlinear processes.

Embedding dimension m, delay time τ, and thresholds ε determine the topological structures of RPs and the indices of RQA. Usually, the number of false newest neighbors is examined to obtain m; τ is obtained via mutual information method, which was proposed by Fraser and Swinney (1986). Following three methods, mean or maximum phase space diameter, recurrence point density, and standard deviation of the observational noise, the appropriate threshold ε can be selected (Marwan et al., 2007).

2.2.2. Measures of dynamic stability

In this study, we chose DET, average diagonal line length (L), entropy (ENTR), and laminarity (LAM) to analyze the dynamic stability of the NDVI series. These five indices were based on the diagonal and vertical line structures of the RPs.

The total number of diagonal lines of length l and number of vertical lines of the length v in the RPs were given by the histograms, respectively:
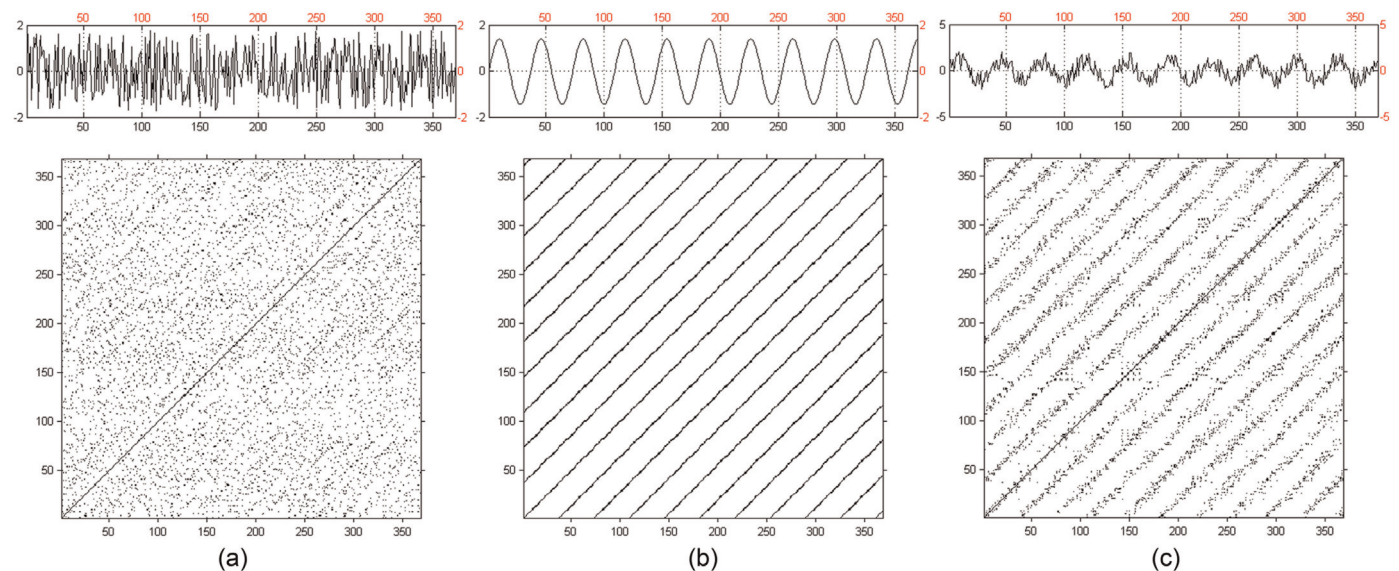

Fig. 2. The RPs of synthetic time series. (a) stochastic series; (b) sine wave series; (c) noise-sinusoidal series. The series length is 387 data points, embedding dimension 4, delay time 6, threshold 0.05.

$$P(l) = \sum_{i,j=1}^{N} \left(1 - R_{i-1\,j-1}(\varepsilon)\right)\left(1 - R_{i+1\,j+1}(\varepsilon)\right)\prod_{k=0}^{l-1}R_{i+k\,j+k}(\varepsilon), \quad (2)$$

$$P(v) = \sum_{i,j=1}^{N} \left(1 - R_{i,j}\right)\left(1 - R_{i,j+v}\right)\prod_{k=0}^{v-1}R_{i,j+k} \quad (3)$$

The diagonal segments represented the predictability time—the time that two trajectories were close before diverging in the state space. And with an appropriately large threshold ε, a large number of the vertical lines usually corresponded to the tangential motion of the phase space trajectory (Marwan et al., 2007).Then, the indices DET, L, ENTR, and LAM were respectively given by

$$DET = \frac{\sum_{l=l_{min}}^{N} lP(l)}{\sum_{i,j}^{N} R_{i,j}}, \quad (4)$$

$$L = \frac{\sum_{l=l_{min}}^{N} lP(l)}{\sum_{l=l_{min}}^{N} P(l)}, \quad (5)$$

$$ENTR = -\sum_{l=l_{min}}^{N} p(l)\ln p(l), \quad (6)$$

$$LAM = \frac{\sum_{v=v_{min}}^{N} vP(v)}{\sum_{v=1}^{N} vP(v)}, \quad (7)$$

where N was the number of points on the phase space trajectory, $P(l)$ and $P(v)$ were histograms of the lengths of diagonal/vertical lines in the RPs.

As Eq. (4) shows, DET is a ratio of recurrence points that form a diagonal structure of all recurrence points, and is a measure of the determinism or predictability of the system. Percent of DET is about zero for a random series and close to 100 for a deterministic series. L represents the average time that two segments of the trajectory are close to each other, and could be interpreted as the mean prediction time. ENTR refers to the Shannon entropy of the probability $p(l) = P(l)/N_l$ to find a diagonal line of exact length l in the RP, and reflects the complexity of the RP in respect to the diagonal lines, with a small ENTR indicating low complexity. LAM represents the occurrence of laminar states in the system without describing the length of the laminar phases, and the value will decrease if the RPs consist of more single recurrence points than vertical structures.

2.3. Datasets

2.3.1. Normalized difference vegetation index

NDVI has been widely used as an estimator of plant productivity and an index for green cover monitoring. This index is computed as the ratio of two electromagnetic wavelengths (near infrared − red)/(near infrared + red). For this study, an NDVI time series of satellite observations at 1 km spatial resolution covering the period from April 1998 to December 2008 were used, via the free VGT

Website (http://free.vgt.vito.be/). The products were produced by SPOT-VEGETATION; vegetation sensors were donated by the European Commission and satellite information came from SPOT-4. The system has been in operation for nearly 15 years, thus offers an unmatched resource for studying vegetation dynamics. In this paper, we used the SPOT-4 VEGETATION ten-day synthesis (called VGT-S10), which was synthesized from S1 (1-day resolution) NDVI products using a maximum value composite algorithm (Jarlan et al., 2008).

2.3.2. Climate data

To more clearly visualize RP structures of the NDVI time series in different climatic regions, six sampling stations were chosen (Table 1; Fig. 1c), representing humid, sub-humid (transition zone), and arid regions, respectively. The information of the six meteorological stations was obtained from the National Meteorological Information Centre, China Meteorological Administration (http://cdc.cma.gov.cn/).

Furthermore, climatic variables were selected to analyze correlation with the RQA indices. Explanatory variables were obtained from the WorldClim Database (Hijmans et al., 2005). This database was a set of global climate layers (climate grids) with a spatial resolution of about 1 km^2, and included monthly total precipitation, and monthly mean, minimum and maximum temperature, and 19 derived bioclimatic variables. Among these variables, four bioclimatic variables representing annual trends (BIO1 = annual mean temperature, BIO12 = annual precipitation) and seasonality (BIO4 = temperature seasonality, BIO15 = precipitation seasonality) were selected to analyze the correlations between climatic factors and RQA indices in this study.

2.4. Analyses

In this study, ArcGIS 9.3 (ESRI Inc., 1999–2008) software was used to perform spatial analysis and produce cartographically appealing maps for RQA indices. The first step transformed the projection of the original SPOT-4 VEGETATION NDVI data into Albers Conical Equal Area projection using Krasovsky 1940 ellipsoid with the central meridian 105°E, first standard parallel 25°N, and second standard parallel 47°N in ArcGIS. Then we extracted the NDVI grid images of the study area using ArcGIS Command Extract by Mask. Next, all NDVI pixel values for each NDVI images were extracted, and the NDVI datasets with matrix size 387 × 30304 were generated. Each NDVI time series (10-day resolution) contained 387 data points, covering the period from April 1998 to December 2008.

After preprocessing the original data, RPs and RQA-based indices were calculated by using CRP Toolbox 5.5 for Matlab by Norbert Marwan (http://tocsy.pik-potsdam.de/CRPtoolbox) . The parameters of RPs and RQA measures were determined by false nearest-neighbor analysis and average mutual information computation, respectively: embedding dimension $m = 4$ and time delay $\tau = 6$. The method for finding the neighbors of the phase space trajectory was a fixed number of nearest neighbors with a threshold ε of 0.5.

Table 1
The geographical characters of sampling meteorology stations.

| Number in Fig. 1c	Code	Site name	Longitude	Latitude	MAT (°C)	MAP (mm)	Climate zone
1	54511	Beijing	116.28°E	39.93°N	12.3	572	Humid region
2	53399	Zhangbei	114.70°E	41.15°N	2.6	382	Transition zone
3	53276	Jurh	112.90°E	42.40°N	4.3	220	Arid region
4	53942	Luochuan	109.50°E	35.82°N	9.2	554	Humid region
5	53725	Dingbian	107.58°E	37.58°N	7.9	321	Transition zone
6	53602	Alxa Zuoqi	105.67°E	38.83°N	7.2	208	Arid region
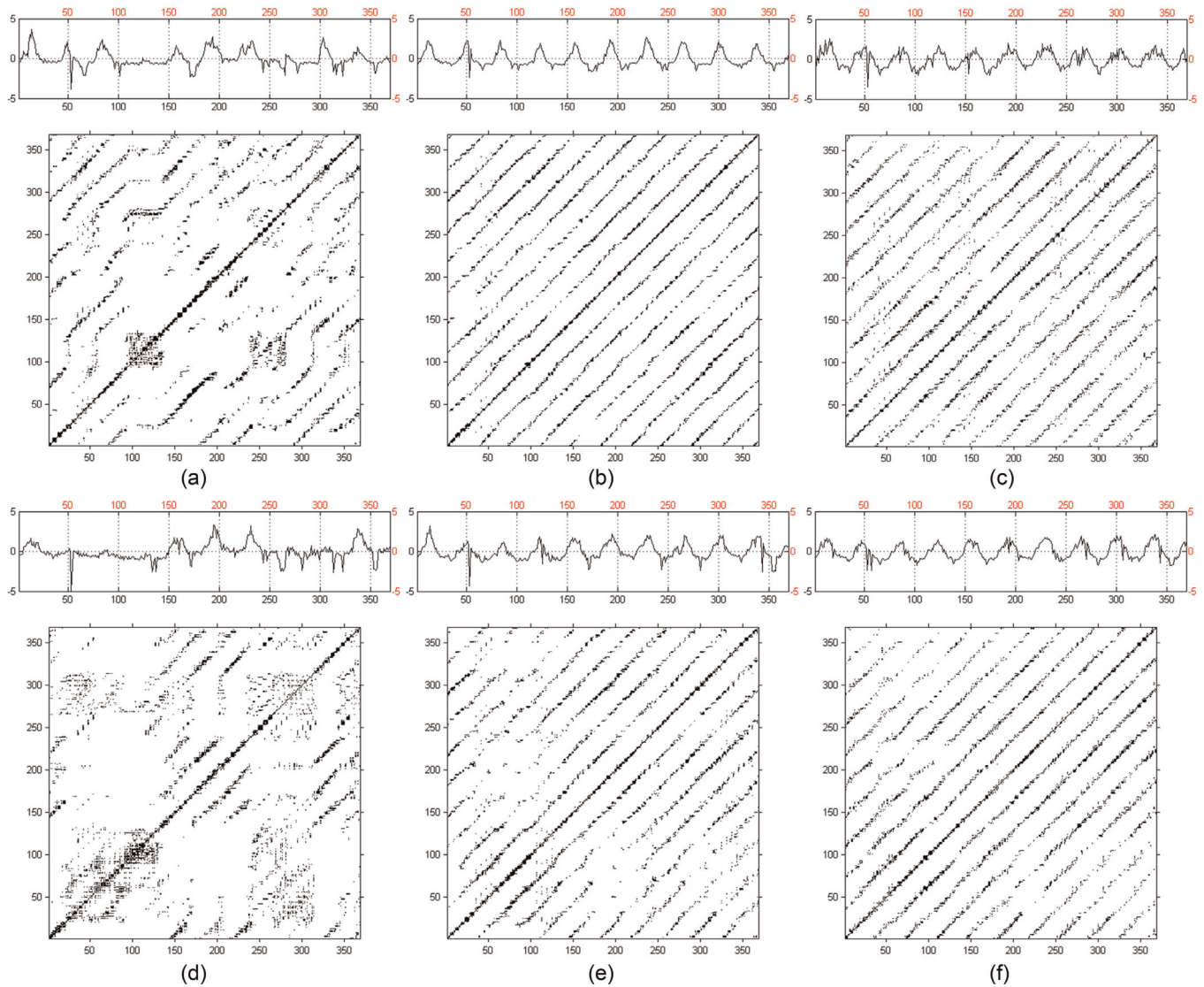
Fig. 3. The RPs of the NDVI series at typical meteorological stations. Dimension: 4, Delay: 6, Threshold: 5% (fixed neighbors amount); (a) 53276, (b) 53399, (c) 54511, (d) 53602, (e) 53725, (f) 53942.

In order to examine the differences in determinism of NDVI time series between transition zones and the surrounding areas, we calculated the average and standard deviation (SD) of the RQA indices. We then analyzed the changes in the RQA indices along the hydrothermal conditions gradient.

3. Results

3.1. RPs at typical meteorological stations

We compared the patterns of the RPs of the NDVI time series at typical meteorological stations. As shown in Fig. 3, the dynamic characteristics of the NDVI series can be differentiated by comparing their RPs, in which the recurrence patterns were significantly different. Compared to Fig. 3c–f, long diagonal lines were rare in Fig. 3a and d, suggesting lower determinism in NDVI series near stations 53,276 and 53,602, which are located at the west side of the transition zone. Only a small proportion of the RPs indicated the NDVI time series presenting recurrence status in these two stations. When comparing the RPs between stations 53,399 and 53,725 in the central part of the transition zone and stations 54,511 and 53,942 at the east side, the patterns seemed

roughly similar with a few minor differences (Fig. 3b vs. c and e vs. f). Despite this, when looking carefully, we can note a significant break-up structure with increasing disturbance frequency in Fig. 3c vs. b, indicating more intensive disturbance was imposed on the NDVI series at station 54,511. Because visual inspection could not distinguish the structures in RPs, the detail must be confirmed by RQA. The RQA indices were calculated for the plots shown in Fig. 3 and given in Table 2.

Table 2
The RQA indices of the NDVI series at typical meteorological stations.

Station	DET	L	ENTR	LAM
53276	0.561	2.721	1.117	0.663
53399	0.643	2.836	1.230	0.689
54511	0.453	2.509	0.950	0.517
53602	0.415	2.608	1.032	0.544
53725	0.538	2.696	1.114	0.643
53942	0.504	2.639	1.066	0.582
Stochastic series[a]	0.079	2.050	0.197	0.094
Periodic series[b]	0.959	11.161	2.204	0.823

[a] Containing pseudorandom values drawn from the standard uniform distribution on the open interval (0,1), obtained by using function rand() in Matlab.
[b] Sinusoidal series, obtained by using function sin() in Matlab.

3.2. Spatial patterns of RQA indices

For each NDVI series in our study area, the RQA indices DET, LAM, ENTR, and L were calculated by Eqs. (4)–(7), and the maps of the results were obtained by using ArcGIS. The statistical values of DET in the whole study area were maximum value 0.82, minimum value 0.10, mean value 0.57, and standard deviation 0.13. The statistical values of LAM were maximum value 0.83, minimum value 0.13, mean value 0.63, and standard deviation 0.11. The statistical values of ENTR were maximum value 1.82, minimum value 0.23, mean value 1.18, and standard deviation 0.22. The statistical values of L were maximum value 4.35, minimum value 2.06, mean value 2.83, and standard deviation 0.29.

As shown in Fig. 4, the spatial patterns of DET, LAM, ENTR, and L presented significant spatial heterogeneity and similar regional distribution in the study area. On the whole, the spatial patterns of recurrence quantity indices (Fig. 4) indicated that higher DET of the NDVI time series occurred in the northeast and middle regions of the study area and lower values in the northwest and south part of the study area. More specifically, at the natural region scale (Table 3), higher RQA index values (for instance, DET > 0.60) occurred in Lesser Xing'an Ranges Changbai mountain coniferous forest region (IIA2), East Songliao plain pediment tableland mixed coniferous broad-leaf forest region (IIA3), Central Songliao plain forest steppe region (IIB1), Central Great Xing'an Ranges mountain forest steppe region (IIB2), West Liao river plain steppe region (IIC1), South Great Xing'an Ranges steppe region (IIC2), East Inner Mongolian plateau steppe region (IIC3), and North China mountain mixed deciduous broad-leaf forest region (IIIB3). However, other

natural regions showed lower RQA indices, which indicated that the NDVI time series showed more irregularity in these areas, especially in the Alxa and Hexi Corridor desert region (IID2) (Table 3).

3.3. RQA indices in transition zone and surrounding areas

In Fig. 4, we can see clearly different characteristics of RQA indices values and spatial distributions between the transition zone and both sides. Therefore, the mean values and standard deviations of DET, LAM, ENTR, and L were counted, as shown in Table 4, to analyze the features of regularity of the NDVI time series in the transition zone that were different from the sides in the study area.

As presented in Table 4, for DET, LAM, ENTR, and L, the transition zone had the highest mean values and lowest variation from the average value among the three parts of the study area, while the east side had lower mean values and higher standard deviation and the west side had the lowest mean values and highest standard deviation. It indicated that the NDVI time series in the transition zone showed more regularity than the surrounding areas.

3.4. Relations between RQA indices and climatic factors

In this study, we discussed the climatic conditions' influences on the spatial patterns of determinism of the NDVI time series. As shown in Fig. 5, we present the scatter plots of DET across the study area, obtaining a visual link between the indices and climatic factors.
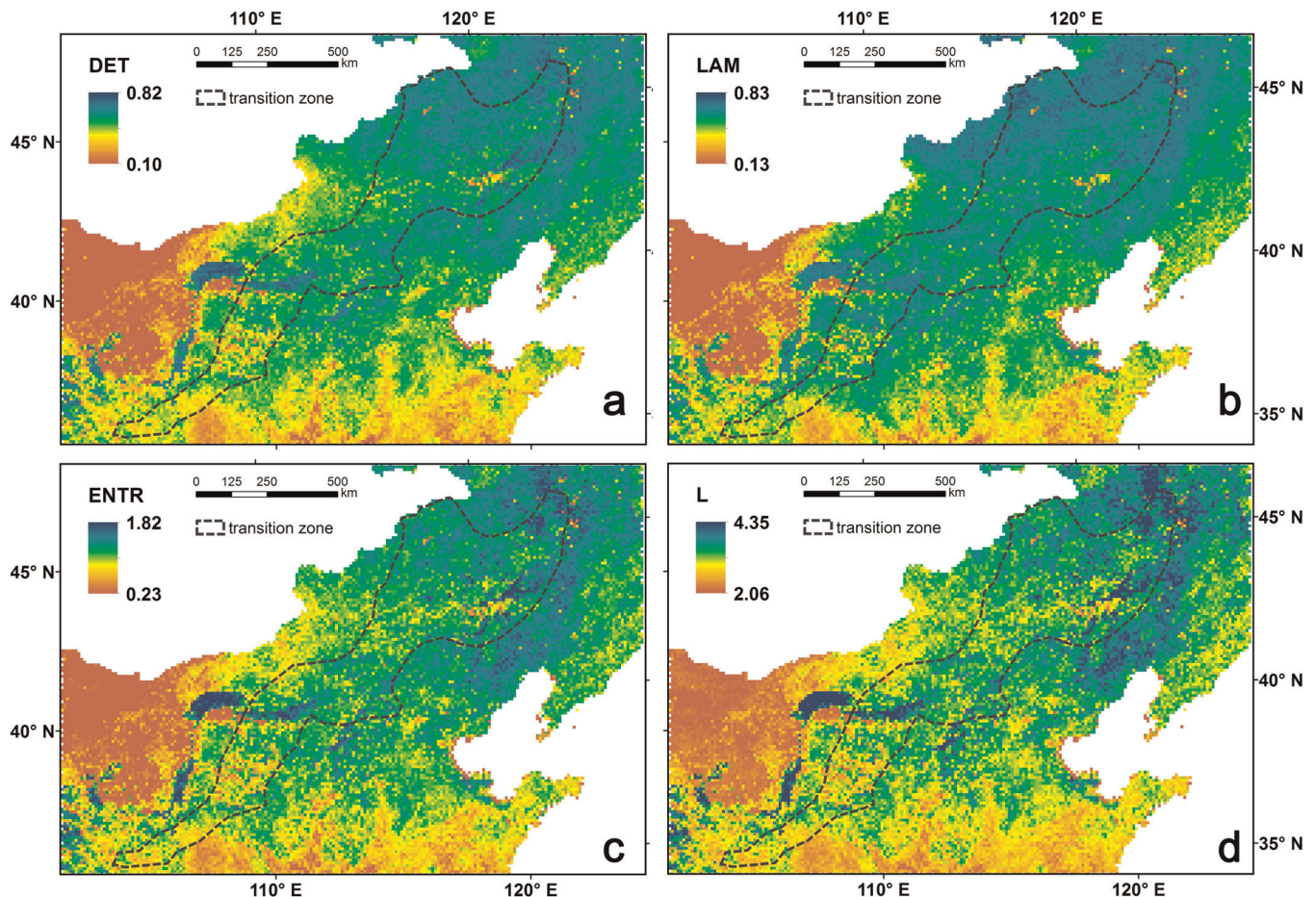

Fig. 4. Spatial patterns of RQA indices. (a) DET; (b) LAM; (c) ENTR; (d) L.

Table 3
The indices of RQA of NDVI series at natural regions.

Code	Natural region	DET	LAM	ENTR	L
IIA2	Lesser Xing'an Ranges Changbai mountain coniferous forest region	0.63	0.65	1.25	2.89
IIA3	East Songliao plain pediment tableland mixed coniferous broad-leaved forest region	0.68	0.70	1.34	3.03
IIB1	Central Songliao plain forest steppe region	0.68	0.73	1.40	3.15
IIB2	Central Great Xing'an Ranges mountain forest steppe region	0.66	0.72	1.33	3.02
IIC1	West Liao river plain steppe region	0.65	0.71	1.32	3.03
IIC2	South Great Xing'an Ranges steppe region	0.67	0.72	1.31	2.99
IIC3	East Inner Mongolian plateau steppe region	0.63	0.71	1.26	2.92
IID1	Ordos and West Inner Mongolian Plateau desert steppe region	0.56	0.65	1.16	2.81
IID2	Alxa and Hexi Corridor desert region	0.34	0.43	0.81	2.43
IIIA1	Liaodong Jiaodong hilly and lower mountain deciduous broad-leaved mixed forest and re-vegetated region	0.55	0.61	1.18	2.78
IIIB1	Luzhong hilly and lower mountain deciduous broad-leaved mixed forest and re-vegetated region	0.48	0.56	1.02	2.60
IIIB2	North China plain re-vegetated region	0.52	0.60	1.13	2.74
IIIB3	North China mountain mixed deciduous broad-leaved forest region	0.62	0.67	1.28	2.94
IIIB4	Fenwei basin deciduous broad-leaved mixed forest and re-vegetated region	0.46	0.56	0.98	2.56
IIIC1	North-central loess plateau steppe region	0.55	0.64	1.15	2.77
HIIC1	Qilian Qingdong mountain basin coniferous forest and steppe region	0.56	0.62	1.18	2.82

The RQA indices values were the mean values in the natural regions.

The data presented in Fig. 5a show a weak negative correlation between DET and annual mean temperature ($R^2 = 0.172$, $P < 0.001$). Using temperature seasonality (standard deviation *100) as a variable, the pattern of the scatter plot was more irregular (Fig. 5b), and DET was weakly positively correlated with the variability of temperature ($R^2 = 0.138$, $P = P < 0.001$). Similarly, as shown in Fig. 5d, it seemed that there was no obvious rule to be followed between DET and precipitation seasonality (coefficient of variation). In contrast, the relations between DET and annual precipitation (Fig. 5c), annual NDVI (Fig. 5e), and aridity index (Fig. 5f) exhibited more obvious regularity. Although the data showed no significant linear correlation between DET and AP, the scatter results indicate that DET first increased and then decreased along with the increasing of AP (Fig. 5c). It is noteworthy that the DET value reached the maximum when the AP is about 400 mm, which is an isohyet boundary between semi-humid monsoon climate and semi-arid continental climate. In addition, transition zones generally locate along the 400 mm isohyet. Parabola fitting was adopted to explore the nonlinear functions between DET and AP, and the model calculation results indicated that the nonlinear relationship was very significant ($R^2 = 0.284$, $P = P < 0.001$). Similar nonlinear relationship displayed between DET and annual NDVI. The nonlinear relationship between DET and the annual NDVI was even more significant ($R^2 = 0.471$, $P = P < 0.001$), calculated by parabola fitting model. The value of DET reached the maximum when the value of NDVI is about 160 (Fig. 5e).

Because of the wide range of MAT and MAP in different regions covered by this study, we adopted aridity index to further explore the influence climatic factors have on DET of NDVI time series (Fig. 5f). The results indicated that DET decreased along with AI increased, the decline followed an exponential pattern ($R^2 = 0.373$,

$P = P < 0.001$), however, the aridity index did not subject to normal distribution and displayed high clustering.

4. Discussions

NDVI time series exhibit cyclic characteristics derived from the plant phenological behaviors. Plant phenological statuses, such as the start of growing season, the rate of biomass accumulation, the rate of vegetation senescence, and the end of growing season, are profoundly influenced by interannual and seasonal climate variations. Meanwhile, the way that vegetation phenology reacts to climate and to socio-economic changes is dependent on the land cover type and on the bioclimatic region (Ivits et al., 2013). Consequently, the spatial characteristic of NDVI time series, associated with plant phenology and vegetation dynamics, has significant heterogeneity, especially in highly heterogeneous areas such as ecogeographical transition zones.

In this study, we revealed spatial variation of the determinism of NDVI time series in North China, and the results indicated that higher determinism of the NDVI time series occurred in the northeast and middle regions and lower values in the northwest and south part of the study area. In addition, transition zones exhibited higher mean values and lower SD in RQA indices than the surrounding areas, which further implies that the NDVI time series in transition zones had more regularity than the NDVI time series in the surrounding areas. The finding is consistent with the previous research of temporal dependence of NDVI series using Hurst exponent (Zhang et al., 2008). The study by Zhang et al. (2008) found that the dynamics of surface vegetation exhibited obvious differences among different land-cover types, and the stability of cultural vegetation and grassland vegetation was lower than the stability of forestland system (Zhang et al., 2008). In our study, relatively higher DET values were found in forest-type regions (DET = 0.623) compared to typical steppe regions (DET = 0.610) and cultural vegetation regions (DET = 0.582).

The remarkable differences in RQA indices could be explained by the diversity in landscape structure and vegetation diversity. In transition zones, one of the major landscape characteristics is alternating distribution of forest patches and steppe patches (Fig. 1d). The scientific premises of landscape ecology suggest that the composition and structure of the landscape mosaic also influence biotic processes and hence influence species richness (Honnay et al., 2003). Many studies have noticed the greater species diversity in transition zones, including the ecotone in North China (Liu et al., 2003). Biodiversity plays an essential role in enhancing system stability; similarly, landscape diversity and

Table 4
The indices of RQA of NDVI series in the transition zone and surrounding areas. An independent-samples t-test was conducted to compare mean values for indices in the transition zone and non-transition zones. There were significant differences ($P < 0.01$) in DET, LAM, ENTR, L, and K_2 between the transition zone and non-transition zones.

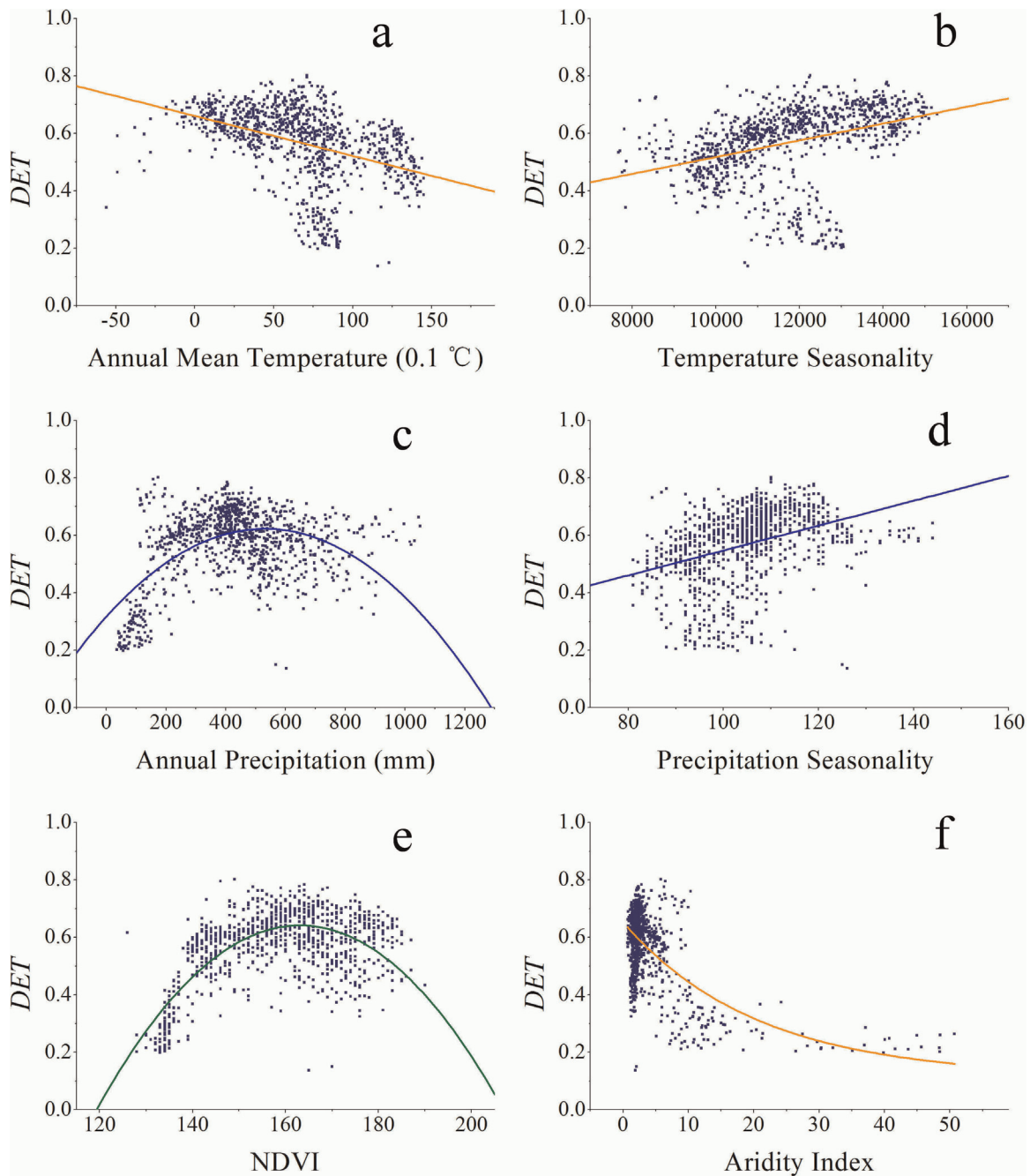| Indices	Transition zone		East side		West side	
	Mean	SD	Mean	SD	Mean	SD
DET	0.631	0.073	0.589	0.097	0.463	0.160
LAM	0.699	0.054	0.651	0.074	0.558	0.151
ENTR	1.268	0.148	1.221	0.178	1.011	0.268
L	2.940	0.231	2.868	0.249	2.645	0.328

SD denotes standard deviation.

Fig. 5. Scatter plots of DET and bioclimatic factors and fitting lines. (a) DET and annual mean temperature; (b) DET and temperature seasonality; (c) DET and annual precipitation; (d) DET and precipitation seasonality; (e) DET and annual NDVI; (f) DET and aridity index.

vegetation diversity result to high adaptive capacity to environmental changes, which explains the high determinism of NDVI time series in transition zones.

Current spatial patterns of vegetation and biodiversity result from long-term natural and anthropogenic process. In our study areas, vegetation patterns are mainly affected by climatic conditions, among which, annual precipitation is the most important factor- the annual precipitation showed a tendency to decline from the southeast to the northwest due to the impact of Pacific monsoon. This may explained the first part of the nonlinear relationship that DET first increased along with the increasing of AP and NDVI before they reach their inflection points, 400 mm and 160, respectively (Fig. 5c and e), during which process, the vegetation types changed from desert steppe, to typical steppe, to

meadow steppe, and to forest-steppe ecotone (Fig. 1d). In addition to climatic conditions, the influence of human activities is also a key factor to vegetation patterns and dynamics. A study of an urbanized region suggested that human disturbance might be the major driving factor for non-stationary dynamic characteristics of NDVI series (Li et al., 2008a). In our study, we found that human activities also influenced the DET spatial patterns of vegetation dynamics. For instance, relatively lower DET values were found in cultural vegetation regions (DET = 0.582) compared to forest-type regions. That is because cropland regions exhibit significant seasonality due to farming activities, with rapid NDVI changes in a short period of three to four months. Besides, agricultural irrigation also affects the distribution and dynamics of NDVI. Human activities cause vegetation dynamics to become relatively

instable and complex, whereas increase biomass and NDVI value. This could explain the decrease of DET with the increasing of AP and NDVI in moist areas (Fig. 5c and e). Landscape homogeneity and plant diversity loss directly influences the structure, function and stability of ecosystems, and the adaptation strategy need to be further studied in future research.

5. Conclusions

Our research focused on the spatial variation of the determinism of NDVI time series in North China, using RPs and RQA methods. The results suggested that remarkable differences of the determinism of NDVI time series exist between transition zones and the surrounding areas. Because the NDVI time series of forests have higher stability than steppes due to longer lag time of vegetation response to climate change, the determinism of NDVI time series is higher in transition zones, where forest patches and steppe patches are alternately distributed. In addition, under the dual influence of climatic and anthropogenic process, the results exhibited a non-linear correlation between determinism of NDVI time series and precipitation and annual NDVI, which is affected by vegetation patterns. Moreover, NDVI time series reached the maximum determinism when the annual precipitation is about 400 mm, which is the lower bound of cultivation and forest distribution, and along the 400 mm isohyet is the area where transition zones locate. The findings of our study will enhance our understandings of transition zones, and will provide methodological reference and technical support for vegetation management.

References

Allan, E., Weisser, W., Weigelt, A., Roscher, C., Fischer, M., Hillebrand, H., 2011. More diverse plant communities have higher functioning over time due to turnover in complementary dominant species. Proc. Natl. Acad. Sci. 108, 17034–17039. doi: http://dx.doi.org/10.1073/pnas.1104015108.

Cui, L., Shi, J., Yang, Y., FAN, W., 2009. Ten-day response of vegetation NDVI to the variations of temperature and precipitation in eastern China. Acta Geographica Sinica 64, 850–860.

Davies, R.G., Orme, C.D.L., Storch, D., Olson, V.A., Thomas, G.H., Ross, S.G., Ding, T.S., Rasmussen, P.C., Bennett, P.M., Owens, I.P.F., 2007. Topography, energy and the global distribution of bird species richness. Proc. Royal Soc. B: Biol. Sci. 274, 1189–1197.

De Mazancourt, C., Isbell, F., Larocque, A., Berendse, F., De Luca, E., Grace, J.B., Haegeman, B., Wayne Polley, H., Roscher, C., Schmid, B., Tilman, D., van Ruijven, J., Weigelt, A., Wilsey, B.J., Loreau, M., 2013. Predicting ecosystem stability from community composition and biodiversity. Ecol. Lett. 16, 617–625. doi:http://dx.doi.org/10.1111/ele.12088 2013.

Eckmann, J.-P., Kamphorst, S.O., Ruelle, D., 1987. Recurrence plots of dynamical systems. EPL (Europhys. Lett.) 4, 973.

Evans, K.L., James, N.A., Gaston, K.J., 2006. Abundance, species richness and energy availability in the North American avifauna. Global Ecol. Biogeogr. 15, 372–385.

Fabretti, A., Ausloos, M., 2005. Recurrence plot and recurrence quantification analysis techniques for detecting a critical regime. Int. J. Mod. Phys. C 16, 671–706.

Fang, J., Piao, S., Tang, Z., Peng, C., Ji, W., 2001. Interannual variability in net primary production and precipitation. Science 293 1723–1723.

Foody, G.M., 2004. Spatial nonstationarity and scale-dependency in the relationship between species richness and environmental determinants for the sub-Saharan endemic avifauna. Global Ecol. Biogeogr. 13, 315–320.

Fraser, A.M., Swinney, H.L., 1986. Independent coordinates for strange attractors from mutual information. Phys. Rev. A 33, 1134.

Gao, J., Li, S., Zhao, Z., Cai, Y., 2012. Investigating spatial variation in the relationships between NDVI and environmental factors at multi-scales: a case study of Guizhou Karst Plateau, China. Int. J. Remote Sens. 33, 2112–2129.

Green, J.L., Hastings, A., Arzberger, P., Ayala, F.J., Cottingham, K.L., Cuddington, K.I.M., Davis, F., Dunne, J.A., Fortin, M.-J., Gerber, L., Neubert, M., 2005. Complexity in ecology and conservation: mathematical, statistical, and computational challenges. BioScience 55, 501–510.

Guo, N., Zhu, Y.J., Wang, J.M., Deng, C.P., 2008. The relationship between NDVI and climate elements for 22 years in different vegetation areas of Northwest China. J. Plant Ecol. 32, 319–327.

Guo, Z., Wang, Z., Song, K., Zhang, B., Li, F., Liu, D., 2007. Correlations between forest vegetation NDVI and water/thermal condition in Northeast China forest regions in 1982–2003. Chinese J. Ecol. 26, 1930–1936.

Hijmans, R.J., Cameron, S.E., Parra, J.L., Jones, P.G., Jarvis, A., 2005. Very high resolution interpolated climate surfaces for global land areas. Int. J. Climatol. 25, 1965–1978.

Honnay, O., Piessens, K., Van Landuyt, W., Hermy, M., Gulinck, H., 2003. Satellite based land use and landscape complexity indices as predictors for regional plant species diversity. Landscape Urban Plann. 63, 241–250.

Jarlan, L., Mangiarotti, S., Mougin, E., Mazzega, P., Hiernaux, P., Le Dantec, V., 2008. Assimilation of SPOT/VEGETATION NDVI data into a sahelian vegetation dynamics model. Remote Sens. Environ. 112, 1381–1394.

Kerr, J.T., Ostrovsky, M., 2003. From space to species: ecological applications for remote sensing. Trends Ecol. Evol. 18, 299–305.

Kottek, M., Grieser, J., Beck, C., Rudolf, B., Rubel, F., 2006. World map of the Koppen–Geiger climate classification updated. Meteorol. Z 15, 259–263.

Li, S.C., Gao, W.M., Zhou, Q.F., Liu, F.Y., 2006a. Multi-scale spatial analysis on NDVI and topographical factors using wavelet transform. Acta Ecologica Sinica 26, 4198–4203.

Li, S.C., Zhou, Q.F., Wu, S.H., Dai, E.F., 2006b. Measurement of climate complexity using sample entropy. Int. J. Climatol. 26, 2131–2139.

Li, S., Zhao, Z., Gao, Y., Wang, Y., 2008a. Determining the predictability and the spatial pattern of urban vegetation using recurrence quantification analysis: a case study of Shenzhen city. Geogr. Res. 27, 1243–1251.

Li, S.C., Zhao, Z.Q., Liu, F.Y., 2008b. Identifying spatial pattern of NDVI series dynamics using recurrence quantification analysis. Eur. Phys. J.-Spec. Topics 164, 127–139.

Li, S.C., Zhao, Z.Q., Wang, Y., Wang, Y.L., 2011. Identifying spatial patterns of synchronization between NDVI and climatic determinants using joint recurrence plots. Environ. Earth Sci. 64, 851–859.

Liu, H., Cui, H., Pott, R., Speier, M., 2000. Vegetation of the woodland-steppe transition at the southeastern edge of the Inner Mongolian Plateau. J. Veg. Sci. 11, 525–532.

Liu, H., Cui, H., 2009. Patterns of plant biodiversity in the woodland-steppe ecotone in southeastern Inner Mongolia. Contemp. Probl. Ecol. 2, 322–329.

Liu, H.Y., Yin, Y., Zhu, J.L., Zhao, F.J., Wang, H.Y., 2010. How did the forest respond to Holocene climate drying at the forest-steppe ecotone in northern China? Quatern. Int. 227, 46–52.

Luo, L., Wang, Z.-M., Song, K.-S., Zhang, B., Liu, D.-W., Ren, C.-Y., Zhang, S.-M., 2009. Research on the correlation between NDVI and climatic factors of different vegetations in the Northeast China. Acta Botanica Boreali-Occidentalia Sinica 29, 800–808.

Marwan, N., Carmen Romano, M., Thiel, M., Kurths, J., 2007. Recurrence plots for the analysis of complex systems. Phys. Rep. 438, 237–329.

Marwan, N., Donges, J.F., Zou, Y., Donner, R.V., Kurths, J., 2009. Complex network approach for recurrence analysis of time series. Phys. Lett. A 373, 4246–4254.

Marwan, N., Kurths, J., 2002. Nonlinear analysis of bivariate data with cross recurrence plots. Phys. Lett. A 302, 299–307.

Marwan, N., Kurths, J., 2005. Line structures in recurrence plots. Phys. Lett. A 336, 349–357.

Marwan, N., Trauth, M.H., Vuille, M., Kurths, J., 2003. Comparing modern and Pleistocene ENSO-like influences in NW Argentina using nonlinear time series analysis methods. Clim. Dynam. 21, 317–326.

Moody, A., Johnson, D.M., 2001. Land-surface phenologies from AVHRR using the discrete fourier transform. Remote Sens. Environ. 75, 305–323.

Onema, J.M.K., Taigbenu, A., 2009. NDVI-rainfall relationship in the Semliki watershed of the equatorial Nile. Phys. Chem. Earth 34, 711–721.

Osborne, P.E., Foody, G.M., Suarez-Seoane, S., 2007. Non-stationarity and local approaches to modelling the distributions of wildlife. Divers. Distrib. 13, 313–323.

Peel, M.C., Finlayson, B.L., McMahon, T.A., 2007. Updated world map of the Koppen–Geiger climate classification. Hydrol. Earth Syst. Sci. Discuss. Discuss. 4, 439–473.

Piao, S., Mohammat, A., Fang, J., Cai, Q., Feng, J., 2006. NDVI-based increase in growth of temperate grasslands and its responses to climate changes in China. Global Environ. Change 16, 340–348.

Piao, S.L., Fang, J.Y., Zhou, L.M., Guo, Q.H., Henderson, M., Ji, W., Li, Y., Tao, S., 2003. Interannual variations of monthly and seasonal normalized difference vegetation index (NDVI) in China from 1982 to 1999. J. Geophys. Res.-Atmos. 108.

Pickett, S.T.A., Cadenasso, M.L., Grove, J.M., 2005. Biocomplexity in coupled natural-human systems: a multidimensional framework. Ecosystems 8, 225–232.

Proulx, R., Côté, P., Parrott, L., 2008. Use of recurrence analysis to measure the dynamical stability of a multi-species community model. Eur. Phys. J. - Spec. Topics 164, 117–126.

Proulx, R., Côté, P., Parrott, L., 2009. Multivariate recurrence plots for visualizing and quantifying the dynamics of spatially extended ecosystems. Ecol. Complex 6, 37–47.

Proulx, R., Wirth, C., Voigt, W., Weigelt, A., Roscher, C., Attinger, S., Baade, J., Barnard, R.L., Buchmann, N., Buscot, F., Eisenhauer, N., Fischer, M., Gleixner, G., Halle, S.,

Hildebrandt, A., Kowalski, E., Kuu, A., Lange, M., Milcu, A., Niklaus, P.A., Oelmann, Y., Rosenkranz, S., Sabais, A., Scherber, C., Scherer-Lorenzen, M., Scheu, S., Schulze, E.-D., Schumacher, J., Schwichtenberg, G., Soussana, J.-F., Temperton, V. M., Weisser, W.W., Wilcke, W., Schmid, B., 2010. Diversity promotes temporal stability across levels of ecosystem organization in experimental grasslands. PLoS ONE 5, e13382. doi:http://dx.doi.org/10.1371/journal.pone.0013382.

Sun, Y., Guo, P., 2012. Variation of vegetation coverage and its relationship with climate change in north China from 1982 to 2006. Ecol. Environ. Sci. 21, 7–12.

Torres, M.E., Gamero, L.G., 2000. Relative complexity changes in time series using information measures. Physica A: Stat. Mech. Appl. 286, 457–473.

Turchin, P., Taylor, A.D., 1992. Complex dynamics in ecological time series. Ecology 73, 289–305.

Udelhoven, T., Stellmes, M., Del Barrio, G., Hill, J., 2009. Assessment of rainfall and NDVI anomalies in Spain (1989–1999) using distributed lag models. Int. J. Remote Sens. 30, 1961–1976.

Von Bloh, W., Romano, M., Thiel, M., 2005. Long-term predictability of mean daily temperature data. Nonlinear Processes Geophys. 12, 471–479.

Wang, J., Xu, X., Liu, P., 1999. Study on land use and population load in inter-distributing area of agricultural and grazing lands in northern China. Resour. Sci. 21, 19–24.

Wang, Z., Guo, Z., Song, K., Luo, L., Zhang, B., Liu, D.-W., Huang, N., Ren, C.-Y., 2009. Response of vegetation NDVI in Northeast China to climate change. Chinese J. Ecol. 28, 1041–1048.

Webber, C.L., Hu, Z., Akar, J., 2011. Unstable cardiac singularities may lead to atrial fibrillation. Int. J. Bifurcation Chaos 21, 1141–1151.

Webber, C.L., Zbilut, J.P., 1994. Dynamical assessment of physiological systems and states using recurrence plot strategies. J. Appl. Physiol. 76, 965–973.

Wu, Y., Li, Z., Wang, Y., Luan, Q., Tian, G., 2009. Responses of vegetation index (NDVI) in typical ecological areas of Shanxi Province to climate change. Chinese J. Ecol. 5, 024.

Xiao, J., Moody, A., 2004. Trends in vegetation activity and their climatic correlates: China 1982 to 1998. Int. J. Remote Sens. 25, 5669–5689.

Xu, X., Chen, H., Zhang, F., 2007. Temporal and spatial change of vegetation cover in the Northwest of China and factors analysis influencing on vegetations variation. Environ. Sci. 28, 41–47.

Zbilut, J.P., Webber Jr., G., 1992. Embeddings and delays as derived from quantification of recurrence plots. Phys. Lett. A 171, 199–203.

Zhang, Xu, X., Zhou, C., Zhang, H., Ouyang, H., 2011. Responses of grassland vegetation to climatic variations on different temporal scales in Hulun Buir Grassland in the past 30 years. J. Geog. Sci. 21, 634–650.

Zhang, X., Hu, Y., Zhuang, D., Qi, Y., 2009. The spatial pattern and differentiation of NDVI in Mongolia Plateau. Geogr. Res.-Aust. 1, 002.

Zhang, Y., Zhao, Z., Li, S., Meng, X., 2008. Indicating variation of surface vegetation cover using SPOT NDVI in the northern part of North China. Geogr. Res.-Aust. 27, 745–755.

Zhao, H.L., Zhao, X.Y., Zhang, T.H., Zhou, R., 2002. Boundary line on agropasture zigzag zone in north China and its problems on ecoenvironment. Adv. Earth Sci. 17, 739–748.

Zhao, Z.Q., Li, S.C., Gao, J.B., Wang, Y.L., 2011. Identifying spatial patterns and dynamics of climate change using recurrence quantification analysis: a case study of qinghai-tibet plateau. Int. J. Bifurcation Chaos 21, 1127–1139.

Zhao, Z.Q., Gao, J.B., Wang, Y.L., Liu, J.G., Li, S.C., 2014. Exploring spatially variable relationships between NDVI and climatic factors in a transition zone using geographically weighted regression. Theor. Appl. Climatol doi:http://dx.doi.org/10.1007/s00704-014-1188-x.

Zheng, D., 2008. Research on Eco-geographical Region Systems of China. The Commercial Press, Beijing.